HHS Public Access

Author manuscript

Mol Cancer Ther. Author manuscript; available in PMC 2020 August 31.

Published in final edited form as:

Mol Cancer Ther. 2012 February ; 11(2): 370–382. doi:10.1158/1535-7163.MCT-11-0458.

DNA Methyltransferase Inhibitor, Zebularine, Delays Tumor Growth and Induces Apoptosis in a Genetically Engineered Mouse Model of Breast Cancer

Min Chen[1,2], **Daniel Shabashvili**[1], **Akbar Nawab**[1], **Sherry X. Yang**[5], **Lisa M. Dyer**[3], **Kevin D. Brown**[3], **Melinda Hollingshead**[6], **Kent W. Hunter**[7], **Frederic J. Kaye**[2], **Steven N. Hochwald**[4], **Victor E. Marquez**[8], **Patricia Steeg**[9], **Maria Zajac-Kaye**[1,2]

[1]Departments of Anatomy and Cell Biology, University of Florida, Gainesville, Florida [2]Departments of Medicine, University of Florida, Gainesville, Florida [3]Departments of Biochemistry and Molecular Biology, University of Florida, Gainesville, Florida [4]Departments of Surgery, University of Florida, Gainesville, Florida [5]Departments of National Clinical Target Validation Laboratory, Bethesda, Maryland [6]Departments of Developmental Therapeutics Program, NCI-Frederick, Bethesda, Maryland [7]Departments of Laboratory of Cancer Biology and Genetics, Bethesda, Maryland [8]Departments of Laboratory of Medicinal Chemistry, Bethesda, Maryland [9]Departments of Laboratory of Molecular Pharmacology, National Cancer Institute, Bethesda, Maryland

Abstract

Zebularine is a novel potent inhibitor of both cytidine deaminase and DNA methylation. We examined the effect of zebularine on mammary tumor growth in genetically engineered MMTV-PyMT transgenic mice that develop mammary tumors at 60 days of age with 100% penetrance. The MMTV-PyMT transgenic mice were randomized at 46 days of age into control ($n = 25$) and zebularine ($n = 25$) treatment groups and monitored for parameters of tumor growth. Zebularine was administered at 5 mg/mL in drinking water. We observed a significant delay in the growth of mammary tumors in zebularine-treated mice with a statistically significant reduction ($P = 0.0135$) in total tumor burden at 94 days of age when the mice were sacrificed. After 48 days of zebularine treatment, the tumors were predominantly necrotic compared with untreated animals. In addition, a high apoptotic index by terminal deoxynucleotidyl transferase–mediated dUTP nick end labeling assay was observed as early as 13 days following treatment. Immunoblot analysis showed depletion of DNMT1 and partial depletion of DNMT3b after zebularine treatment. Microarray analyses of global gene expression identified upregulation of twelve methylation-regulated genes as well as a set of candidate cancer genes that participate in cell growth and apoptosis. In summary, zebularine inhibits the growth of spontaneous mammary tumors and causes early onset of tumor cell necrosis and apoptosis in a genetically engineered mouse model of breast cancer.

Corresponding Author: Maria Zajac-Kaye, University of Florida, College of Medicine, Cancer and Genetics Research Complex, Room 360, 2033 Mowry Rd, Gainesville, FL 32610. Phone: 352-273-9153; Fax: 352-273-8299; mzajackaye@ufl.edu.

Disclosure of Potential Conflicts of Interest

No potential conflicts of interest were disclosed.

Note: Supplementary material for this article is available.

Defining the parameters of zebularine-mediated tumor inhibition may advance the future development of DNA methyltransferase inhibitors as an effective cancer treatment.

Introduction

Hypermethylation is commonly detected within the promoter and other regulatory regions of many cancer-associated genes in primary tumor biopsies and derived tumor cell lines (1). Because aberrant hypermethylation is associated with reversible gene silencing, the development of pharmacologic inhibitors of DNA methylation has provided a rational approach for cancer therapy. Specific inhibitors of DNA methylation such as 5-azacytidine (aza-CR) and its deoxy analog, 5-Aza-2′deoxycytidine (5-Aza-CdR) have been studied for decades, however, both drugs are toxic *in vitro* and *in vivo*, and have been difficult to administer due to their low stability in aqueous solution (2–4).

Zebularine is a novel DNA methyltransferase (DNMT) inhibitor, which was developed as a more stable and less toxic drug (5). Zebularine, similar to aza-CR and 5-Aza-CdR, incorporates into DNA and forms a covalent irreversible complex with DNMTs (6) preventing the enzyme from methylating position 5 of cytosines clustered in regulatory CpG islands. Recent studies showed the ability of zebularine to sustain the demethylation state of the 5′ region of the tumor suppressor gene *CDKN2A/p16* and other methylated genes in T24, HCT15, CFPAC-1, SW48, and HT-29 cells (6). It was also reported that zebularine inhibits growth of cancer cell lines but not normal cells (7). A recent study showed that zebularine treatment inhibited the growth of lung tumor cells with hypermethylated *CDKN2A* gene while it had no effect on lung cancer cells with homozygous deletion of *CDKN2A* (8), suggesting a link with reactivation of *CDKN2A*. In addition, oral or intraperitoneal administration of zebularine in the EJ6 bladder cancer xenograft model in nude mice reduced tumor growth with minimal toxicity (9).

In this study, the antitumor growth effect of zebularine was investigated using a genetically engineered mouse model (GEMM) that develops mammary tumors within 60 days with 100% penetrance. MMTV-PyMT transgenic mice express polyomavirus middle T antigen and develop spontaneous multifocal mammary tumors with a rapid conversion of mammary epithelium to the malignant state (10). Epigenetic silencing of tumor suppressor and growth regulatory genes has been implicated in breast cancer (11–15) and dysregulated DNA methyltransferase activity may also be a contributing factor to breast cancer development (16). Therefore, to determine the ability of zebularine to prevent or treat breast cancer, we tested if daily oral treatment with zebularine affects mammary tumor growth in these MMTV-PyMT mice. We observed a significant delay in tumor growth and a reduction of total tumor burden in the zebularine-treated mice. We also showed depletion of DNMTs in tumors excised from zebularine-treated mice and identified upregulation of 12 genes previously characterized as silenced by DNA hypermethylation. A microarray analysis of RNA extracted from excised mammary tumors from zebularine-treated and control mice also identified a set of dysregulated genes that function in cell cycle, apoptosis, cell growth, and signaling pathways that correspond to genes previously shown to play a role in tumor formation in MMTV-PyMT mice. Finally, we showed that zebularine treatment resulted in

the induction of necrosis and apoptosis in spontaneously developed tumors with no apparent toxicity to the mice.

Materials and Methods

Animals

Female FVB/N-Tg(MMTV-PyMT)^{634Mul} mice were housed in filter-topped cages and provided autoclaved feed *ad libitum*. Mice were monitored 3 times each week for tumor occurrence. Because this strain of transgenic mouse develops tumors in all 10 mammary glands, the first tumor to grow in an anterior gland (glands 1, 2, 3, 6, 7, and 8) was monitored as the axillary tumor and the first tumor to develop in a posterior gland (glands 4, 5, 9, and 10) was monitored as the inguinal tumor. When tumors became palpable, perpendicular diameter measurements of each tumor were collected every 2 to 3 days with calipers, and the volumes were calculated using the formula (L × W × W)/2. Tumor weight for the axillary and the inguinal tumors were calculated for the treated and control group of mice (n = 10 per group). The total tumor burden was compared by Student t test for the control and the treated animals. The normal mammary glands 2 and 3 or gland 4 were dissected from an age-matched (70 days old) normal FVB/N mouse, and DNA, RNA, and protein extracts were prepared as described below. All animal studies were conducted in accordance with the principles and procedures outlined in the USPHS Guidelines for the Care and Use of Laboratory Animals in an Association Assessment and Accreditation of Laboratory Animal Care International-approved facility under an approved animal protocol.

Drug treatment *in vivo*

For the zebularine treatment, the mice were treated via drinking water by solubilizing zebularine at 5 mg/mL in water. To encourage consumption, sucrose was added to the drinking water at 2 g/100 mL. Vehicle control mice received sucrose-supplemented drinking water. Prior animal studies (17) with zebularine showed that daily i.p. doses in excess of 900 mg/kg were tolerated. To study a protracted course of daily zebularine, we selected drinking water as a clinically relevant and less stressful way to provide continuous exposure. Based upon the typical mouse water consumption rate of 150 mL of water per kg of body weight, we elected to administer the agent at 5 mg/mL of water thereby producing a daily zebularine dose of 750 mg/kg.

In addition to quantitate zebularine levels in the mice, plasma samples were collected from mice undergoing treatment with zebularine via the drinking water (5 mg/mL) at 7, 14, and 21 days of treatment (n = 3 per time point). Samples were found to contain average zebularine levels of 9.56, 16.0, and 31.8 μmol/L at days 7, 14, and 21, respectively. This shows that zebularine does accumulate with chronic dosing via the drinking water. Untreated controls (n = 10) had zebularine levels of 0 μmol/L. Zebularine was provided by the Drug Synthesis and Chemistry Branch, Developmental Therapeutics Program, NCI.

Histologic evaluation

Tumor tissues collected from zebularine-treated and untreated animals were stored at −80° C. For slide preparation, a small piece of tumor was excised and frozen tumors were

transferred from −80° C to −20° C overnight. Tumor tissues were fixed for 24 hours in 10% formaldehyde solution, transferred to 70% ethanol, and embedded in paraffin. Sections were cut (5 μm) and mounted on salinated slides for hematoxylin and eosin (H&E) staining (Histoserv Inc). Tumor necrosis was evaluated by 2 investigators on H&E–stained slides.

Terminal deoxynucleotidyl transferase-mediated dUTP nick end labeling

The terminal deoxynucleotidyl transferase-mediated dUTP nick end labeling (TUNEL) assay (R&D Systems) was conducted on formalin-fixed and paraffin-embedded sections as previously described (18). An avidin-conjugated horseradish peroxidase bound to the biotinylated DNA fragments was used to generate a brown precipitate in the presence of diamenobezidine (Vector Laboratories Inc.). A nuclease-treated tumor specimen section was used as a positive control, and the same tumor section without nuclease treatment was used as a negative control. Tumor apoptosis was analyzed quantitatively by Automated Cellular Imaging System (ACIS; Dako) as described previously (19). A hot spot feature of the ACIS was used to identify sites of apoptotic labeling where 6 areas of tumor were scored with a 40× tool or a free-scoring tool. The instrument calculated an average labeling percentage.

Immunoblot analysis

Excised tumor was resuspended in 1 mL of RIPA buffer containing protease inhibitors as recommended by the manufacturer (Santa Cruz Biotech; Kit # sc-24948). Tumors were cut with scissors to small pieces and were homogenized for 30 to 60 seconds to disperse the tissue. Cell extracts were incubated on ice for 1 hour and centrifuged at full speed in a microcentrifuge. The supernatant was aliquoted and stored at −80° C. Thirty micrograms of protein extract was resolved by SDS-PAGE, transferred to nitrocellulose membrane, and immuno-blotted with anti-DNMT1-antibody (clone 60B1220; Abcam) at 2 μg/mL and with DNMT3b antibody (Novus Biological, catalog # NB100–266) 1:1,000 dilution as previously described (20). The α-tubulin antibody (clone DM1A) was purchased from Sigma and used in 1:1,000 dilution as loading control.

Microarray gene expression hybridization and validation by real-time reverse transcriptase PCR

RNA was isolated from 9 axillary tumor tissues that were excised at 13, 23, and 48 days (3 animals were used for each time point) and from 9 matched tumors excised from the untreated control animals. Total RNA was isolated by TRIzol reagent (Invitrogen) according to the standard protocol, followed by DNase treatment and RNA cleanup (RNeasy Mini Kit; QIAGEN). RNA integrity was determined by the RNA 6000 Nano LabChip Kit on Agilent 2100 Bioanalyzer (Agilent Technologies). cRNA from the MMTV-PyMT tumors was hybridized to the Affymetrix GeneChip Mouse Genome 430 2.0 Arrays, scanned with an Affymetrix GeneChip scanner 3000, and analyzed with Microarray Suite 5.0 software (MAS5; Affymetrix Inc.). Mean signal intensity was scaled to a target value of 500 using all probe sets. Normalization, gene filtering, comparative gene expression, and hierarchical clustering analysis were done with BRB Array Tools software developed by the Biometric Research Branch of the National Cancer Institute. The genes for all analyses were filtered by requiring the spot intensity to be more than 10. Each array was normalized using the median over the entire array. Only genes that reported values in at least 75% of the samples were

included for further analysis. The Class Comparison Tool, using Univariate Two-Sample T-test with random variance model and permutations of the class labels was applied to all probes that passed the signal intensity and missing value filters. A total of 868 genes (representative of 1.8% genes) with a minimum 1.5-fold expression change in either direction from the median value of the gene ($P < 0.05$) with the signal intensity more than 200 were selected. Overrepresentation analysis was conducted by EASE software. Expressed genes in the ontology terms having EASE score less than 0.05 were selected. The Gene Ontology (GO) terms were ranked by the significance of overrepresentation. This model takes into account not only the relative changes (i.e., fold change), but also the absolute expression, thereby cleaning up relatively "noisy" data from very weakly expressed genes.

Quantitative real-time reverse transcriptase (RT)-PCR analyses were conducted on the iCycler iQ real-time PCR detection system (BioRad Laboratories) using the TaqMan EZ RT-PCR CORE Reagent Kit (Applied Biosystems) according to the manufacturers recommendation. Analysis of each sample was carried out in triplicates, using cDNA as template for PCR amplification. For quantitation of gene expression, the endogenous reference 18s rRNA was used to normalize the difference between samples. Specific hybridization probes for mouse 18s rRNA and the genes of interest labeled with 5-FAM reporter dye were purchased from Applied Biosystems.

Pyrosequencing analysis

Sodium bisulfite conversion of 1 μg of genomic DNA harvested from normal murine mammary epithelium and mammary tumor specimens was carried out with the EZ DNA Methylation-Direct Kit (Zymo Research Corporation) according to the manufacturer's protocol. PCR amplification of the lower DNA strand was conducted in a 20-μL reaction volume containing 1 × Coral buffer (QIAGEN), 250 nmol/L deoxynucleotides, 250 nmol/L each of forward and reverse biotinylated primers, 1 U of HotStarTaq Plus DNA polymerase (QIAGEN) and 1 μL (50–100 ng) of bisulfite-treated DNA. Amplification conditions were as follows: one cycle at 95° C for 5 minutes followed by 40 cycles at 95° C for 30 seconds, 50° C to 52° C for 30 seconds, 72° C for 30 seconds, and a final extension step at 72° C for 10 minutes. Prior to pyrosequencing, PCR products were analyzed by agarose gel electrophoresis/ethidium bromide staining. Pyrosequencing was conducted in a mixture of 5 to 10 μL of PCR product with 2 μL of streptavidin-coated sepharose beads (GE Healthcare Bio-Sciences AB) and 40 μL of binding buffer (10 mmol/L Tris-HCl, 2 mol/L NaCl, 1 mmol/L EDTA, 0.1% Tween 20, pH 7.6) brought up to 80 μL total volume with distilled H_2O. This mixture was immobilized on streptavidin beads by shaking constantly at 1400 rpm for 10 minutes at room temperature (RT). The beads were harvested with a vacuum preparation workstation and appropriate sequencing primer added to a final concentration of 330 nmol/L. The sequencing primers were annealed to the template by incubating the samples at 80° C for 2 minutes and cooled at RT for 10 minutes prior to analysis. Primer sequences for *Twist2* were TGGAtAATAAGATGAttAGt-TGtAGt for the forward primer (also used as the sequencing primer) and tAAGttAGGGTAGGTGtTG for the reverse primer (lower case indicates bisulfite-converted cytosines). Pyrosequencing was conducted with a

PyroMark MD system (QIAGEN), and sequence analysis conducted with the supplied Pyro Q-CpG software by Biotage AB.

Statistical analysis

The significance of the comparisons between different treatment groups was determined by Student *t* test. Statistical analysis of tumor burden was conducted with the nonparametric Mann–Whitney *U* test.

Results

Oral administration of zebularine delays tumor development and reduces tumor burden in transgenic MMTV-PyMT mice

Female transgenic MMTV-PyMT mice spontaneously develop palpable mammary gland tumors at approximately 60 days of age. Mammary tumors were separated into anterior (axillary) and posterior (inguinal) tumors. To examine the effect of oral zebularine (Fig. 1A) on mammary tumors, we randomly assigned 46-day-old mice to control ($n = 25$) and zebularine ($n = 25$) treatment groups (Fig. 1B). Tumors were measured every 2 to 3 days, and tumor volume was calculated as described in the Materials and Methods. Only the first axillary and inguinal tumors to arise were used for measurements. The average tumor volume for the mammary tumors (one axillary and one inguinal tumor per mouse) was calculated for each group ($n = 10$ mice for each group). We observed a 10-day delay in the onset of palpable tumor growth in zebularine-treated mice, which was statistically significant (Fig. 1C, $P < 0.05$). When axillary and inguinal tumors were examined separately, we observed a 7- and 12-day delay, respectively, in the onset of palpable axillary and inguinal mammary tumors in zebularine-treated mice (Fig. 1D, $P < 0.05$ and 1E, $P < 0.01$). Mice were treated up to 94 days of age (total of 48 days of zebularine treatment) at which time the mice were sacrificed and the total tumor burden was excised and weighed. We also found a statistically significant reduction in total tumor burden in zebularine-treated mice as compared with control mice at 94 days of age (Fig. 1F, $P = 0.0135$).

Zebularine treatment induces necrosis and apoptosis in mammary gland tumors

To determine the effect of zebularine on tumor growth, we first examined the morphology of tumors in treated and control mice. After 48 days of zebularine treatment, areas of tumor necrosis (acellular pink staining region) comprised about 50% of the tissue section (Fig. 2A, images a and c). In contrast, poorly differentiated mammary tumor cells without necrosis were observed in the untreated animals (Fig. 2A, images b and d). This data suggest that tumor cell death induced by zebularine treatment may have contributed to the delay in detectable tumor growth in mice. To confirm that cell death was a result of induction of apoptosis, we carried out a TUNEL assay on tumors derived from zebularine-treated and untreated control animals. Apoptotic cells were observed as early as 13 days after zebularine treatment (Fig. 2B). At day 13, a high percentage of apoptotic cells were observed in tumors examined in all 4 mice treated with zebularine (10%, 11%, 56%, and 84%; Fig. 2C). A negligible level of apoptotic cells was found in tumors derived from 4 control animals (0%, 1.6%, 2.0%, and 2.2%; Fig. 2C, $P = 0.057$). At day 48, all 3 tumors derived from the zebularine-treated animals showed a high apoptotic index (Fig. 2C), whereas a significantly

lower apoptotic index was found in tumors derived from 3 control animals tested (Fig. 2C, $P < 0.05$).

Depletion of DNMT1a and DNMT3b protein levels by zebularine

Because it has been shown that zebularine treatment of tumor cell lines resulted in depletion of DNMT1 and a partial depletion of DMNT3b *in vitro* (7), we set out to determine if zebularine treatment depletes DNMT1 and DNMT3b within tumors *in vivo*. Using immunoblot analysis of protein extract from tumors isolated from zebularine-treated mice or from untreated mice, we observed a near complete depletion of DNMT1 and a partial depletion of DMNT3b 23 days after zebularine treatment (Fig. 3A and B). We found that tumors derived from all 3 zebularine-treated mice examined showed a near complete depletion of DMNT1 (Fig. 3A, lanes 4–6) as compared with tumors from untreated animals that contain high level of DNMT1 protein (Fig. 3A, lanes 1–3 and Fig. 3C, lanes 4 and 5). In addition, 2 of 3 zebularine-treated animals show depletion of DMNT3b (Fig. 3B, lanes 4–6) as compared with tumors from untreated animals that contain high level of DNMT3b protein (Fig. 3B, lanes 1–3 and Fig. 3C, lanes 4 and 5). The levels of DNMT1 and DNMT3b returned to normal after 48 days of treatment (data not shown) perhaps due to outgrowth of tumor cells resistant to zebularine treatment.

We also compared the levels of DNMT1 and DNMT3b in normal mammary glands versus mammary tumors. We found that levels of DNMT1 and DNMT3b are lower in normal mammary glands (Fig. 3C, lanes 1–3) as compared with high levels observed in untreated tumors (Fig. 3A, lanes 1–3 and B, lanes 1–3 and Fig. 3C, lanes 4 and 5) suggesting that DNMT1 and DNMT3b are induced during tumorigenesis in MMTV-PyMT mice.

Alteration of global gene expression by zebularine treatment

To identify potential molecular pathways involved in the delay of tumor development by zebularine treatment, we compared the global gene mRNA expression profiles between tumors isolated from untreated and zebularine-treated mice at day 13 ($n = 3$), day 23 ($n = 3$), and day 48 ($n = 3$). We detected 868 genes differentially expressed at these time points in zebularine-treated versus untreated samples. This included 194 genes that were upregulated and 188 genes downregulated at 13 days after treatment (Supplementary Tables S1 and S2), 100 genes upregulated and 120 genes downregulated 23 days after treatment (Supplementary Tables S3 and S4), and 158 genes upregulated and 108 genes downregulated 48 days after treatment (Supplementary Tables S5 and S6). In this data set, we included only genes that were at least 1.5-fold differentially regulated and for which statistical significance ($P < 0.05$) was reached.

To search for cancer relevant signaling pathways altered by zebularine treatment *in vivo*, we used EASE software (http://EaseSoftware.com) and classification of 868 genes by KEGG database (http://www.genome.jp/kegg) and GO (http://www.geneontology.org). We found that zebularine treatment significantly regulated expression of genes that are involved in DNA methylation, apoptosis, cell cycle, tumor suppression, and metastasis. Further, altered expression of components of the Akt, Src, and Ras cancer signaling pathways (Table 1 and 2) was also observed. We also noted that 12 genes previously characterized as regulated by

aberrant hypermethylation were upregulated by zebularine treatment (1.5- to 2.4-fold) when compared with untreated controls (Table 1). Specifically, we observed increased expression of CCND2/cyclin D2, CDKN1A/p21, lamin A, Sfrp1, Becn1, Twist2, prostaglandin 2 (Ptgs2), H19, Myod1, gelsolin (Gsn), Igfbp6, and TGFβi (full names and gene IDs are shown in Table 1). In addition, 2 genes regulated by DNA methylation, Wif1 (11) and HDAC11 (21), were downregulated 3.2- and 1.5 fold respectively (Table 2).

Because it has been previously reported that expression of the cell-cycle regulator Cdc25C was increased in MMTV-PyMT tumors (22), we also examined the effect of zebularine on the expression of cell cycle–regulated genes as a mechanism for tumor growth inhibition. As expected, we observed that after zebularine treatment, Cdc25C and other genes required for cell proliferation such as CDK4 and Cdc20, were downregulated (Table 2), whereas tumor suppressor genes such as CDKN1A, Becn1, and Sfrp1 were upregulated (Table 1). In addition, expression of apoptosis-related genes such as Casp4, Sfrp1, and Igfbp6 were also upregulated (Table 1). We also found that zebularine-treated MMTV-PyMT mice showed an increased Ptgs2 expression in tumors after 23 days of treatment, which correlated with increased Sfrp1 expression 48 days after treatment. This is an interesting observation because Sfrp1 promotes apoptosis (23) and was shown to be induced 38-fold following Ptgs2 treatment of osteoblasts (24).

Molecular analysis of tumors arising in MMTV-PyMT transgenic mice showed activation of phosphatidylinositol 3-kinase (PI3K; refs. 25, 26), Src (27), and Ras (28) signaling pathways. Our microarray profile revealed that genes involved in the tumorigenic PI3K/Akt signaling pathways that are associated with MMTV-PyMT tumor formation, such as Akt1, PIK3cd, and PIK3c2a (29), were downregulated by zebularine treatment (Table 1 and Supplementary Table S1). In addition, genes involved in Src and Ras signaling such as Catns, Rasal1, Tnfrsf19, and Tnfrsf11a were also downregulated after 13 and 23 days of zebularine treatment (Table 2 and Supplementary Tables S2 and S4). Matrix metalloprotease (MMP) family members previously shown to be increased in PyMT tumors (30) were also downregulated by zebularine treatment. Moreover, Gsn, considered to be a favorable prognostic factor for erbB2-positive breast cancer patients (31) and known to be downregulated in MMTV-PyMT tumors (22) was found to be upregulated by zebularine treatment. Thus, the expression of a large cassette of previously identified genes that function in tumor formation in MMTV-PyMT mice was affected by zebularine treatment.

We selected 6 genes from the microarray gene list for validation with quantitative real-time reverse transcription PCR. These genes were chosen because their expression was either known to be regulated by aberrant hypermethylation or because they play a direct role in the regulation of DNA methylation. H19, CDKN1A, and Ptgs2 were upregulated in the microarray analysis and were confirmed to be upregulated by real-time RT-PCR analysis (Fig. 4A). Wif1 was downregulated in microarray analysis and this was confirmed by real-time RT-PCR (Fig. 4A). In addition, the expression of DNMT3b was downregulated 1.3-fold in the microarray analysis although it is not listed in Table 1 because the cutoff was 1.5-fold downregulation in selecting our data set (Fig. 4A). Altered expression of only 2 genes (*HIF-1* and *DAPK1*), which were downregulated 1.5-fold in microarray analysis, could not be confirmed by real-time RT-PCR analysis (data not shown). The expression levels of *H19,*

CDKN1A and *Ptgs2, Wif1* and *DNMT3b* genes, as detected by microarray and real-time RT-PCR were highly correlated with $R^2 = 0.94$ (Fig. 4B).

Comparison of gene silencing and methylation status between normal mammary glands, mammary tumors, and tumors from zebularine-treated mice

We measured mRNA expression by quantitative real-time RT-PCR for Sfrp1, Twist2, CDKN1A, Becn1, and H19 in normal mammary gland, mammary tumors, and mammary tumors from zebularine-treated MMTV-PyMT mice. When compared with normal mammary gland tissues, Sfrp1, Twist2, CDKN1A, Becn1, and H19 were each found to be dramatically downregulated in tumor specimens (Fig. 5A and Supplementary Table S7). Moreover, compared with day 69 tumor specimens, increases in Sfrp1, CDKN1A, Becn1, and H19 expression levels were measured in mammary tumors dissected from 69-day-old MMTV-PyMT mice treated with zebularine for 23 days (Fig. 5A and Supplementary Table S7). Consistent with microarray results, upregulation of Twist2 was observed in mammary tumors from 94-day-old zebularine-treated MMTV-PyMT mice (48 days of treatment), whereas no upregulation of Twist2 in tumors dissected from 69-day-old (23 days of treatment) zebularine-treated mice was observed (Supplementary Table S7).

To investigate the correlation of DNA methylation in silencing and reactivation of Twist2 expression in normal mammary glands (glands 2 and 3 and gland 4 measured separately), mammary tumors, and tumors in mice treated with zebularine, the methylation status of the *Twist2* gene was determined. Specifically, pyrosequencing was used to quantitatively measure cytosine methylation at 4 distinct CpG dinucleotides within the dense CpG island present at the mouse *Twist2* locus (Fig. 5B). We measured low *Twist2* methylation at each of the 4 CpG sites interrogated in normal mammary gland tissues (3.8% average overall; Fig. 5C). At each CpG site, we also measured increased CpG methylation in mammary tumor samples (16.4% average overall, $P < 0.05$). After zebularine treatment, average CpG methylation was significantly reduced to 9.6%. When taken together, a clear correlation was evident between gene methylation and mRNA expression for *Twist2* gene in normal mammary gland and mammary tumors from untreated and zebularine-treated MMTV-PyMT mice.

Discussion

We have shown that the DNA methylation inhibitor, zebularine, has antitumor effects in a genetically engineered breast cancer mouse model. We found that zebularine treatment caused a significant delay of tumor formation and induced necrosis and apoptosis in mammary tumors that developed in MMTV-PyMT transgenic mice. GEMMs recapitulate many aspects of human cancer and more closely resemble tumor histology and microenviromental features of naturally occurring cancers (32) than the more common xenograft model system. Moreover, recent studies show that GEMMs predicted clinical trial outcomes when standard chemotherapy either alone or in combination with targeted agents was used (33). Because xenograft models do not reliably predict human clinical outcomes (34), GEMMs may lay a framework for predicting outcomes by studying therapeutic response and drug resistance. In this study, we chose the MMTV-PyMT GEMM (25) as

these mice develop mammary tumors with a 100% incidence rate. As DNA methylation seems to play an important role in modulation of cancer-associated genes in sporadic breast cancer (11–13, 15, 35, 36), this GEMM provided a powerful model to test the efficacy of the novel methylation inhibitor, zebularine. Zebularine treatment was shown to be associated with a dose-dependent depletion of DNMT1, DNMT3a, and DNMT3b proteins in the breast cancer cell lines MCF-7 and MDA-MB-231 (37). Zebularine also depletes DNMT1 in T24 bladder carcinoma cells after 24 hours of treatment and partially depletes DNMT3b after 3 days of drug exposure (7). Our *in vivo* study confirmed that DNMT1 was depleted, and DNMT3b was significantly lowered (50% depletion) in the mammary tumors derived from zebularine-treated mice as compared with untreated mice. This would result in loss of steadystate levels of methylated DNA and induction of genes that could contribute to the antitumor effect observed in zebularine-treated animals. In addition, we observed low levels of DNMT1 and DMNT3b expression in normal mammary gland from FVB/N mice. Expression of DNMT1 and DMNT3b was significantly increased in mammary tumors. These findings may highlight a mechanism that could contribute to epigenetic dysregulation in MMTV-PyMT mice.

We observed that a panel of 5 genes (Twist2, Becn1, Sfrp1, Cdkn1a, and H19), identified in our expression microarray screen as upregulated in zebularine-treated tumors (Table 1), showed detectable levels of mRNA expression in normal axillary (glands #2 and 3) and inguinal (gland #4) mammary glands from FVB/N mice. Furthermore, expression of each of these genes was significantly downregulated in mammary tumors. This is consistent with the epigenetic silencing of these genes in mammary tumors that develop in MMTV-PyMT mice model. Moreover, treatment of these mice with zebularine increased expression of each of these genes. Detailed analysis of DNA methylation by pyrosequencing analysis revealed that zebularine treatment resulted in a decreased level of CpG methylation within the *Twist2* promoter. When taken together, we conclude that zebularine induces DNA demethylation within mammary tumors arising in PyMT mice and promotes reexpression of epigenetically silenced genes within these tumors.

Using a microarray screening approach, we detected a total of 12 candidate genes (Table 1) previously reported to be regulated by DNA hypermethylation that were upregulated in the excised mammary tumors of our zebularine-treated mice. These included CCND2/cyclin D2, CDKN1A/p21, lamin A, Sfrp1, Becn1, Twist2, Ptgs2, H19, Myod1, Gsn, Igfbp6, and TGFβi. Reexpression of Sfrp1, CDKN1A, Becn1, Ptgs2, and Igfbp6 was associated with loss of the DNMT1 in mouse fibroblasts (38). Interestingly, the hypermethylated *Sfrp1* gene can also be induced by 5-aza-deoxycytidine. This drug causes inhibition of the transformed phenotype in breast (13) and gastrointestinal cancers (39–41). In addition, zebularine treatment induced CCND2/cyclin D2, an important regulator of the G_1–S cell-cycle transition. Cyclin D2 mRNA and protein are absent in breast cancer cell lines and in primary breast cancers, whereas cultured normal breast epithelial cells had abundant expression (42–44). The fact that cyclin D2 expression is silenced by hypermethylation in human breast tumors and our observation that zebularine induced cyclin D2 gene expression in mammary GEMM tumors suggests that induction of cyclin D2 may participate in breast tumor growth inhibition.

CDKN1A/p21, known to be activated after DNA damage to arrest cell growth (45, 46) was also upregulated in MMTV-PyMT mice tumors after 23 days of zebularine treatment confirming previous observations that CDKN1A/p21 was induced by zebularine in MCF-7 breast cancer cells (47). We did not observe, however, the reactivation of *CDKN2A/p16* gene in tumors derived from zebularine-treated MMTV-PyMT mice. *CDKN2A/p16* gene was found previously to be activated by zebularine in nonbreast human cancer cell lines (6–9). Although CDKN2A/p16 was shown to be hypermethylated in 5 out of 16 breast cancer tissue samples, and in 1 out of 6 breast cancer cell lines, there are no reports in literature indicating induction of p16 mRNA or protein levels by demethylating agents in breast cancer cells (48). In summary, zebularine, a known DNMT inhibitor, depletes DNMTs *in vivo* and reactivates (at least) 12 genes silenced by aberrant DNA hypermethylation in a breast cancer mouse model.

We also observed that zebularine treatment altered the expression of genes that are involved in cell proliferation, cell-cycle regulation, apoptosis, and signaling. In summary, genes that are required for cell proliferation (Cdc25C, CDK4, and Cdc20) were downregulated (Table 2), whereas tumor suppressor genes that undergo tumor-specific hypermethylation (CDKN1A, Becn1, and Sfrp1) were upregulated (Table 1). Zebularine treatment also resulted in apoptotic cell death, which was associated with upregulation of Casp4, Sfrp1, and CDKN1A (Table 1). The apoptosis and tumor necrosis induced by zebularine treatment may have contributed to the delay in tumor growth in MMTV-PyMT transgenic mice. Although we do not know which combination of the zebularine-regulated genes may have directly contributed to delay of tumor growth, we do notice that the same genes that are reexpressed by zebularine treatment have been found to induce apoptosis and inhibit tumor cell growth in breast cancer (13, 49–52). It remains to be determined which of these genes might play a direct role in the inhibition of the tumor growth and induction of apoptosis in MMTV-PyMT mice treated by zebularine.

The mechanism of tumor formation in MMTV-PyMT transgenic mice has been well characterized and reported to involve the activation of PI3K/Akt (25, 26), Src (27) and Ras (22, 28) pathways. PyMT binds PI3K to activate downstream effectors of PI3K/Akt (26), and a recent finding shows that Akt1 ablation delays the development of mammary adenocarcinomas in MMTV-PyMT mice (53). The results from our microarray profile revealed that Akt1 and other genes involved in this pathway such as Pik3cd and Pik3c2a were downregulated by zebularine treatment (Table 1 and Supplementary Table S1). In addition, we showed that proteins such as Catns, Rasal1, Tnfrsf19 (22), and Tnfrsf11a, each of which function in Src and Ras signaling, were differentially downregulated following zebularine treatment (Table 2 and Supplementary Tables S2 and S4). In addition, Cdc25C, a critical cell-cycle regulator, and metalloproteases, MMP-2, MMP-3, and MMP-13, were increased in MMTV-PyMT tumors (22, 30). We found that expression of Cdc25C and other cell-cycle regulators including Cdc20 and CDK4 as well as expression of MMP-12 and MMP-13 was downregulated in zebularine-treated MMTV-PyMT mammary tumors. Moreover, expression of Gsn was found to be decreased in PyMT tumors (22). Gsn is widely expressed by normal cells and downregulated in many tumor types, including breast cancer (54), and was shown to have tumor-suppressive activity (54, 55). Consistent with these observations, Gsn was upregulated by zebularine treatment in the MMTV-PyMT mice.

Therefore, it is not surprising that tumor growth was delayed in zebularine-treated MMTV-PyMT mice because the genes that are known to play a role in the PyMT tumorgenesis were affected by zebularine treatment.

Zebularine has been reported to prevent early tumor development and also to inhibit growth of already established tumor cells. For example, zebularine was shown to prevent intestinal tumors in cancer prone$^{APCmin/+}$ mice (56) and to induce apoptosis in pancreatic cancer models (57), myeloid leukemia cells (58), breast cancer cells (37), and in the MMTV-PyMT mammary gland tumors as shown in our experiments. In addition, oral or intraperitoneal administration of zebularine in the EJ6 bladder cancer xenograft model reduced tumor growth in nude mice (9). Regardless of the mechanism of tumor growth inhibition, tumor cells eventually develop resistance to zebularine treatment. Because it has been shown that zebularine and the HDAC inhibitor depsipeptide have a synergistic effect on the inhibition of lung and breast cancer growth (8) a combinatorial treatment with DNA methyltransferase inhibitors and HDAC inhibitors may be warranted to overcome resistance to single-drug therapy.

Supplementary Material

Refer to Web version on PubMed Central for supplementary material.

Acknowledgments

The authors thank Diana Nguyen, Luanne Lukes, Donna Voeller, and Di Hua He for technical assistance. The authors also thank Chandramouli Gadisetti and Carolyn Best for microarray analysis.

Grant Support

This work was supported by National Cancer Institute intramural program and by the Department of Medicine and Department of Anatomy and Cell Biology at the University of Florida.

References

1. Jones PA, Baylin SB. The epigenomics of cancer. Cell 2007;128: 683–92. [PubMed: 17320506]
2. Jones PA, Taylor SM. Cellular differentiation, cytidine analogs and DNA methylation. Cell 1980;20:85–93. [PubMed: 6156004]
3. Sorm F, Vesely J. Effect of 5-aza-2′-deoxycytidine against leukemic and hemopoietic tissues in AKR mice. Neoplasma 1968;15:339–43. [PubMed: 5684460]
4. Beisler JA. Isolation, characterization, and properties of a labile hydrolysis product of the antitumor nucleoside, 5-azacytidine. J Med Chem 1978;21:204–8. [PubMed: 74412]
5. Yoo CB, Cheng JC, Jones PA. Zebularine: a new drug for epigenetic therapy. Biochem Soc Trans 2004;32:910–2. [PubMed: 15506921]
6. Cheng JC, Yoo CB, Weisenberger DJ, Chuang J, Wozniak C, Liang G, et al. Preferential response of cancer cells to zebularine. Cancer Cell 2004;6:151–8. [PubMed: 15324698]
7. Cheng JC, Weisenberger DJ, Gonzales FA, Liang G, Xu GL, Hu YG, et al. Continuous zebularine treatment effectively sustains demethylation in human bladder cancer cells. Mol Cell Biol 2004;24:1270–8. [PubMed: 14729971]
8. Chen M, Voeller D, Marquez VE, Kaye FJ, Steeg PS, Giaccone G, et al. Enhanced growth inhibition by combined DNA methylation/HDAC inhibitors in lung tumor cells with silenced CDKN2A. Int J Oncol 2010;37:963–71. [PubMed: 20811718]

9. Cheng JC, Matsen CB, Gonzales FA, Ye W, Greer S, Marquez VE, et al. Inhibition of DNA methylation and reactivation of silenced genes by zebularine. J Natl Cancer Inst 2003;95:399–409. [PubMed: 12618505]
10. Guy CT, Cardiff RD, Muller WJ. Induction of mammary tumors by expression of polyomavirus middle T oncogene: a transgenic mouse model for metastatic disease. Mol Cell Biol 1992;12:954–61. [PubMed: 1312220]
11. Ai L, Tao Q, Zhong S, Fields CR, Kim WJ, Lee MW, et al. Inactivation of Wnt inhibitory factor-1 (WIF1) expression by epigenetic silencing is a common event in breast cancer. Carcinogenesis 2006;27:1341–8. [PubMed: 16501252]
12. Lo PK, Mehrotra J, D'Costa A, Fackler MJ, Garrett-Mayer E, Argani P, et al. Epigenetic suppression of secreted frizzled related protein 1 (SFRP1) expression in human breast cancer. Cancer Biol Ther 2006;5:281–6. [PubMed: 16410723]
13. Yang ZQ, Liu G, Bollig-Fischer A, Haddad R, Tarca AL, Ethier SP. Methylation-associated silencing of SFRP1 with an 8p11–12 amplification inhibits canonical and non-canonical WNT pathways in breast cancers. Int J Cancer 2009;125:1613–21. [PubMed: 19569235]
14. Periyasamy S, Ammanamanchi S, Tillekeratne MP, Brattain MG. Repression of transforming growth factor-beta receptor type I promoter expression by Sp1 deficiency. Oncogene 2000;19:4660–7. [PubMed: 11030155]
15. Suzuki H, Toyota M, Carraway H, Gabrielson E, Ohmura T, Fujikane T, et al. Frequent epigenetic inactivation of Wnt antagonist genes in breast cancer. Br J Cancer 2008;98:1147–56. [PubMed: 18283316]
16. Girault I, Tozlu S, Lidereau R, Bieche I. Expression analysis of DNA methyltransferases 1, 3A, and 3B in sporadic breast carcinomas. Clin Cancer Res 2003;9:4415–22. [PubMed: 14555514]
17. Dote H, Cerna D, Burgan WE, Carter DJ, Cerra MA, Hollingshead MG, et al. Enhancement of in vitro and in vivo tumor cell radiosensitivity by the DNA methylation inhibitor zebularine. Clin Cancer Res 2005;11:4571–9. [PubMed: 15958643]
18. Nagler RM, Kerner H, Ben-Eliezer S, Minkov I, Ben-Itzhak O. Prognostic role of apoptotic, Bcl-2, c-erbB-2 and p53 tumor markers in salivary gland malignancies. Oncology 2003;64:389–98. [PubMed: 12759537]
19. Yang SX, Steinberg SM, Nguyen D, Wu TD, Modrusan Z, Swain SM. Gene expression profile and angiogenic marker correlates with response to neoadjuvant bevacizumab followed by bevacizumab plus chemotherapy in breast cancer. Clin Cancer Res 2008;14:5893–9. [PubMed: 18794102]
20. Beaulieu N, Morin S, Chute IC, Robert MF, Nguyen H, MacLeod AR. An essential role for DNA methyltransferase DNMT3B in cancer cell survival. J Biol Chem 2002;277:28176–81.
21. Bradbury CA, Khanim FL, Hayden R, Bunce CM, White DA, Drayson MT, et al. Histone deacetylases in acute myeloid leukaemia show a distinctive pattern of expression that changes selectively in response to deacetylase inhibitors. Leukemia 2005;19:1751–9. [PubMed: 16121216]
22. Qiu TH, Chandramouli GV, Hunter KW, Alkharouf NW, Green JE, Liu ET. Global expression profiling identifies signatures of tumor virulence in MMTV-PyMT-transgenic mice: correlation to human disease. Cancer Res 2004;64:5973–81. [PubMed: 15342376]
23. Melkonyan HS, Chang WC, Shapiro JP, Mahadevappa M, Fitzpatrick PA, Kiefer MC, et al. SARPs: a family of secreted apoptosis-related proteins. Proc Natl Acad Sci U S A 1997;94:13636–41.
24. Bodine PV, Billiard J, Moran RA, Ponce-de-Leon H, McLarney S, Mangine A, et al. The Wnt antagonist secreted frizzled-related protein-1 controls osteoblast and osteocyte apoptosis. J Cell Biochem 2005;96:1212–30. [PubMed: 16149051]
25. Webster MA, Hutchinson JN, Rauh MJ, Muthuswamy SK, Anton M, Tortorice CG, et al. Requirement for both Shc and phosphatidylinositol 3′ kinase signaling pathways in polyomavirus middle T-mediated mammary tumorigenesis. Mol Cell Biol 1998;18:2344–59. [PubMed: 9528804]
26. Whitman M, Kaplan DR, Schaffhausen B, Cantley L, Roberts TM. Association of phosphatidylinositol kinase activity with polyoma middle-T competent for transformation. Nature 1985;315:239–42. [PubMed: 2987699]

27. Webster MA, Cardiff RD, Muller WJ. Induction of mammary epithelial hyperplasias and mammary tumors in transgenic mice expressing a murine mammary tumor virus/activated c-src fusion gene. Proc Natl Acad Sci U S A 1995;92:7849–53. [PubMed: 7544006]
28. Srinivas S, Schonthal A, Eckhart W. Polyomavirus middle-sized tumor antigen modulates c-Jun phosphorylation and transcriptional activity. Proc Natl Acad Sci U S A 1994;91:10064–8.
29. Castaneda CA, Cortes-Funes H, Gomez HL, Ciruelos EM. The phosphatidyl inositol 3-kinase/AKT signaling pathway in breast cancer. Cancer Metastasis Rev 2010;29:751–9. [PubMed: 20922461]
30. Pedersen TX, Pennington CJ, Almholt K, Christensen IJ, Nielsen BS, Edwards DR, et al. Extracellular protease mRNAs are predominantly expressed in the stromal areas of microdissected mouse breast carcinomas. Carcinogenesis 2005;26:1233–40. [PubMed: 15760918]
31. Thor AD, Edgerton SM, Liu S, Moore DH 2nd, Kwiatkowski DJ. Gelsolin as a negative prognostic factor and effector of motility in erbB-2-positive epidermal growth factor receptor-positive breast cancers. Clin Cancer Res 2001;7:2415–24. [PubMed: 11489821]
32. Olive KP, Tuveson DA. The use of targeted mouse models for preclinical testing of novel cancer therapeutics. Clin Cancer Res 2006;12:5277–87. [PubMed: 17000660]
33. Singh M, Lima A, Molina R, Hamilton P, Clermont AC, Devasthali V, et al. Assessing therapeutic responses in Kras mutant cancers using genetically engineered mouse models. Nat Biotechnol 2010;28:585–93. [PubMed: 20495549]
34. Gopinathan A, Tuveson DA. The use of GEM models for experimental cancer therapeutics. Dis Model Mech 2008;1:83–6. [PubMed: 19048065]
35. Dobrovic A, Simpfendorfer D. Methylation of the BRCA1 gene in sporadic breast cancer. Cancer Res 1997;57:3347–50. [PubMed: 9269993]
36. Fackler MJ, McVeigh M, Mehrotra J, Blum MA, Lange J, Lapides A, et al. Quantitative multiplex methylation-specific PCR assay for the detection of promoter hypermethylation in multiple genes in breast cancer. Cancer Res 2004;64:4442–52. [PubMed: 15231653]
37. Billam M, Sobolewski MD, Davidson NE. Effects of a novel DNA methyltransferase inhibitor zebularine on human breast cancer cells. Breast Cancer Res Treat 2010;120:581–92. [PubMed: 19459041]
38. Jackson-Grusby L, Beard C, Possemato R, Tudor M, Fambrough D, Csankovszki G, et al. Loss of genomic methylation causes p53-dependent apoptosis and epigenetic deregulation. Nat Gen 2001;27: 31–9.
39. Zou H, Molina JR, Harrington JJ, Osborn NK, Klatt KK, Romero Y, et al. Aberrant methylation of secreted frizzled-related protein genes in esophageal adenocarcinoma and Barrett's esophagus. Int J Cancer 2005;116:584–91. [PubMed: 15825175]
40. Suzuki H, Watkins DN, Jair KW, Schuebel KE, Markowitz SD, Chen WD, et al. Epigenetic inactivation of SFRP genes allows constitutive WNT signaling in colorectal cancer. Nat Gen 2004;36: 417–22.
41. Nojima M, Suzuki H, Toyota M, Watanabe Y, Maruyama R, Sasaki S, et al. Frequent epigenetic inactivation of SFRP genes and constitutive activation of Wnt signaling in gastric cancer. Oncogene 2007;26: 4699–713. [PubMed: 17297461]
42. Evron E, Umbricht CB, Korz D, Raman V, Loeb DM, Niranjan B, et al. Loss of cyclin D2 expression in the majority of breast cancers is associated with promoter hypermethylation. Cancer Res 2001;61: 2782–7. [PubMed: 11289162]
43. Fischer H, Chen J, Skoog L, Lindblom A. Cyclin D2 expression in familial and sporadic breast cancer. Oncol Rep 2002;9:1157–61. [PubMed: 12375011]
44. Sweeney KJ, Sarcevic B, Sutherland RL, Musgrove EA. Cyclin D2 activates Cdk2 in preference to Cdk4 in human breast epithelial cells. Oncogene 1997;14:1329–40. [PubMed: 9178893]
45. Waldman T, Kinzler KW, Vogelstein B. p21 is necessary for the p53-mediated G1 arrest in human cancer cells. Cancer Res 1995;55: 5187–90. [PubMed: 7585571]
46. el-Deiry WS, Harper JW, O'Connor PM, Velculescu VE, Canman CE, Jackman J, et al. WAF1/CIP1 is induced in p53-mediated G1 arrest and apoptosis. Cancer Res 1994;54:1169–74. [PubMed: 8118801]

47. Macleod KF, Sherry N, Hannon G, Beach D, Tokino T, Kinzler K, et al. p53-dependent and independent expression of p21 during cell growth, differentiation, and DNA damage. Genes Dev 1995;9: 935–44. [PubMed: 7774811]

48. Herman JG, Merlo A, Mao L, Lapidus RG, Issa JP, Davidson NE, et al. Inactivation of the CDKN2/p16/MTS1 gene is frequently associated with aberrant DNA methylation in all common human cancers. Cancer Res 1995;55:4525–30. [PubMed: 7553621]

49. Chopin V, Slomianny C, Hondermarck H, Le Bourhis X. Synergistic induction of apoptosis in breast cancer cells by cotreatment with butyrate and TNF-alpha, TRAIL, or anti-Fas agonist antibody involves enhancement of death receptors' signaling and requires P21(waf1). Exp Cell Res 2004;298:560–73. [PubMed: 15265702]

50. Choi EJ, Kim GH. Apigenin causes G(2)/M arrest associated with the modulation of p21(Cip1) and Cdc2 and activates p53-dependent apoptosis pathway in human breast cancer SK-BR-3 cells. J Nutr Biochem 2009;20:285–90. [PubMed: 18656338]

51. Liang XH, Jackson S, Seaman M, Brown K, Kempkes B, Hibshoosh H, et al. Induction of autophagy and inhibition of tumorigenesis by beclin 1. Nature 1999;402:672–6. [PubMed: 10604474]

52. Ramachandran C, Rodriguez S, Ramachandran R, Raveendran Nair PK, Fonseca H, Khatib Z, et al. Expression profiles of apoptotic genes induced by curcumin in human breast cancer and mammary epithelial cell lines. Anticancer Res 2005;25:3293–302. [PubMed: 16101141]

53. Maroulakou IG, Oemler W, Naber SP, Tsichlis PN. Akt1 ablation inhibits, whereas Akt2 ablation accelerates, the development of mammary adenocarcinomas in mouse mammary tumor virus (MMTV)-ErbB2/neu and MMTV-polyoma middle T transgenic mice. Cancer Res 2007;67:167–77. [PubMed: 17210696]

54. Asch HL, Head K, Dong Y, Natoli F, Winston JS, Connolly JL, et al. Widespread loss of gelsolin in breast cancers of humans, mice, and rats. Cancer Res 1996;56:4841–5. [PubMed: 8895730]

55. Vandekerckhove J, Bauw G, Vancompernolle K, Honore B, Celis J. Comparative two-dimensional gel analysis and microsequencing identifies gelsolin as one of the most prominent downregulated markers of transformed human fibroblast and epithelial cells. J Cell Biol 1990;111:95–102. [PubMed: 2164032]

56. Yoo CB, Chuang JC, Byun HM, Egger G, Yang AS, Dubeau L, et al. Long-term epigenetic therapy with oral zebularine has minimal side effects and prevents intestinal tumors in mice. Cancer Prev Res (Phila Pa) 2008;1:233–40.

57. Neureiter D, Zopf S, Leu T, Dietze O, Hauser-Kronberger C, Hahn EG, et al. Apoptosis, proliferation and differentiation patterns are influenced by Zebularine and SAHA in pancreatic cancer models. Scand J gastroenterology 2007;42:103–16.

58. Scott SA, Lakshimikuttysamma A, Sheridan DP, Sanche SE, Geyer CR, DeCoteau JF. Zebularine inhibits human acute myeloid leukemia cell growth *in vitro* in association with p15INK4B demethylation and reexpression. Exp Hematol 2007;35:263–73. [PubMed: 17258075]

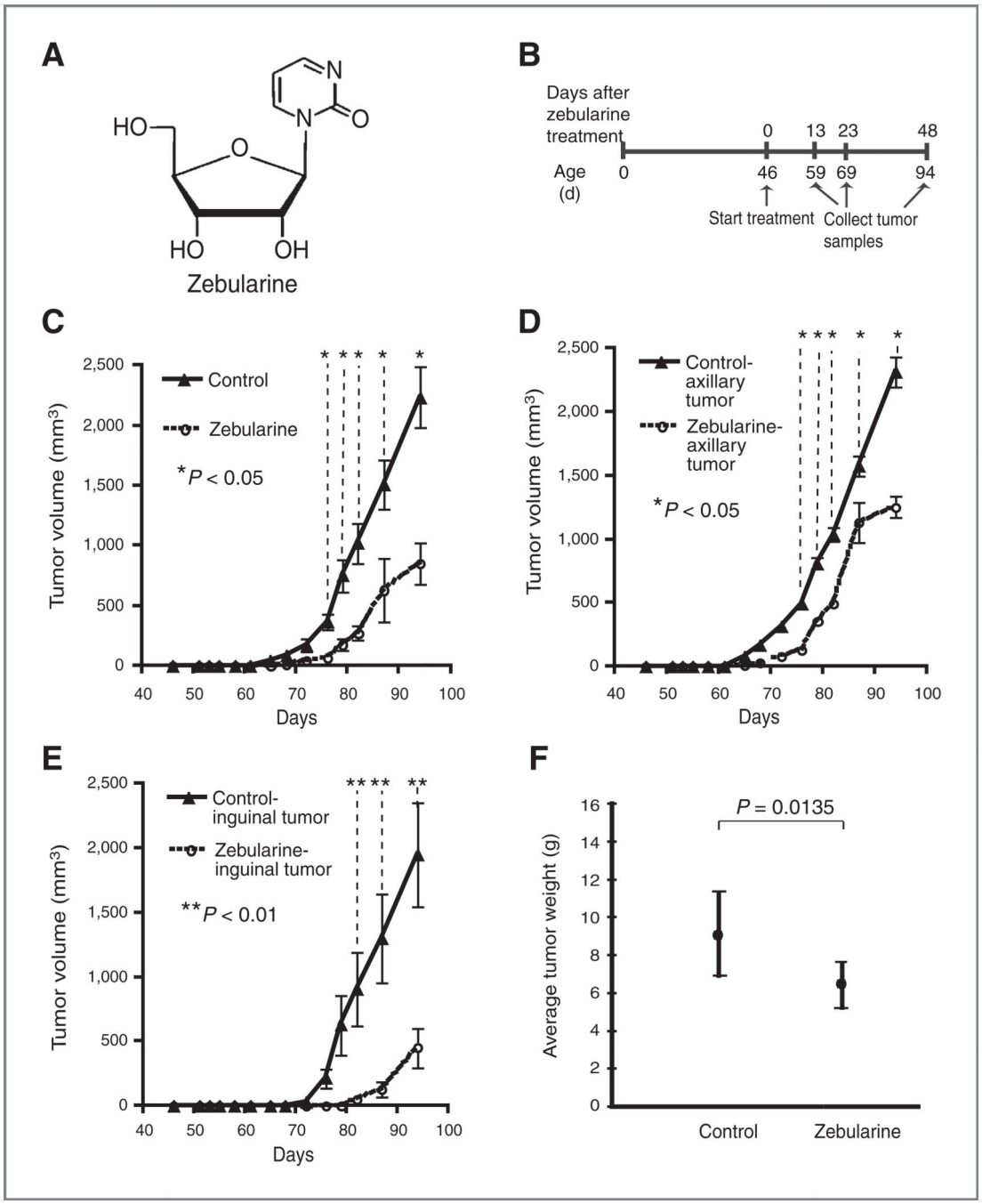

Figure 1.

Effect of zebularine on tumor growth in MMTV-PyMT transgenic mice. A, chemical structure of zebularine. B, schematic representation of zebularine treatment. Cohorts of female MMTV-PyMT mice ($n = 50$) were monitored for onset of palpable mammary tumors and size of the tumor. At 46 days of age, the mice were randomized into control and zebularine-treated groups ($n = 25$ each). For zebularine treatment, mice were treated via solubilizing 5 mg/mL zebularine in sucrose-supplemented water. Control mice received sucrose-supplemented drinking water. C and D, delay of tumor growth in zebularine-treated

mice. C, the average tumor volume for both axillary and the inguinal tumors were calculated for zebularine-treated (n = 10) or control (n = 10) mice. The data for the first axillary and first inguinal tumors is shown. D, the average tumor volume for axillary tumors was calculated for zebularine-treated (n = 10) or control (n = 10) mice. Only the data for the first axillary tumor detected in each animal are shown. E, the average tumor volume for inguinal tumors were calculated for zebularine-treated (n = 10) or control (n = 10) mice. Only the data for the first inguinal tumor detected are shown. Triangles and circles represent mean tumor volume for control and zebularine-treated mice, respectively. Bars represent SD. F, ten mice in each group were treated to 94 days of age at which time they were sacrificed, and the total tumor burden was excised and weighed and presented as mean ± SD. The total tumor burden for the control and treated animals was compared by Student t test. P values are shown in C to F.

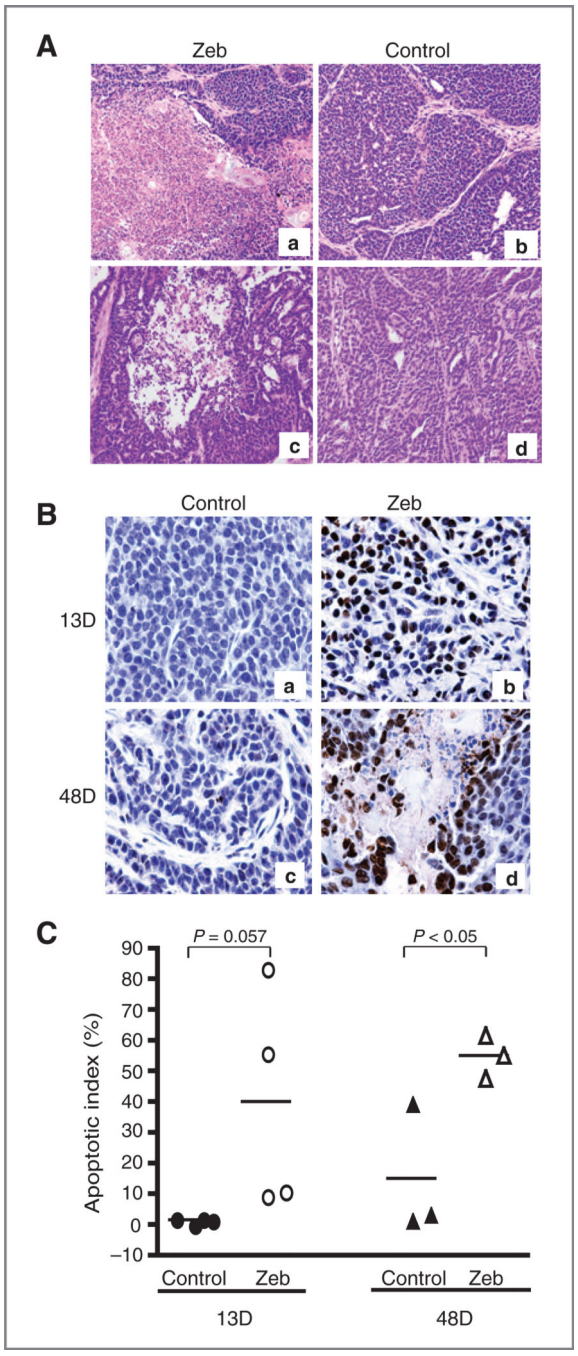

Figure 2.

Effect of zebularine treatment on tumor necrosis and apoptosis in MMTV-PyMT transgenic mice. A, extensive necrosis characterized by acellular pink area was detected in 50% of section after 48 days of zebularine treatment (a and c). Negligible necrosis in control animals (b and d). Magnification, ×200. B, TUNEL assay revealed extensive apoptotic cells in mammary tumors after 13 and 48 days of zebularine treatment (b and d). Negligible level of apoptotic cells detected in untreated tumors (a and c). C, quantitative analysis of apoptotic cells with Automated Cellular Imaging System shows a higher apoptotic index after 13 (n =

4 mice) and 48 days (n = 3 mice) of zebularine treatment compared with the untreated tumor. P value is indicated. Zeb, zebularine.

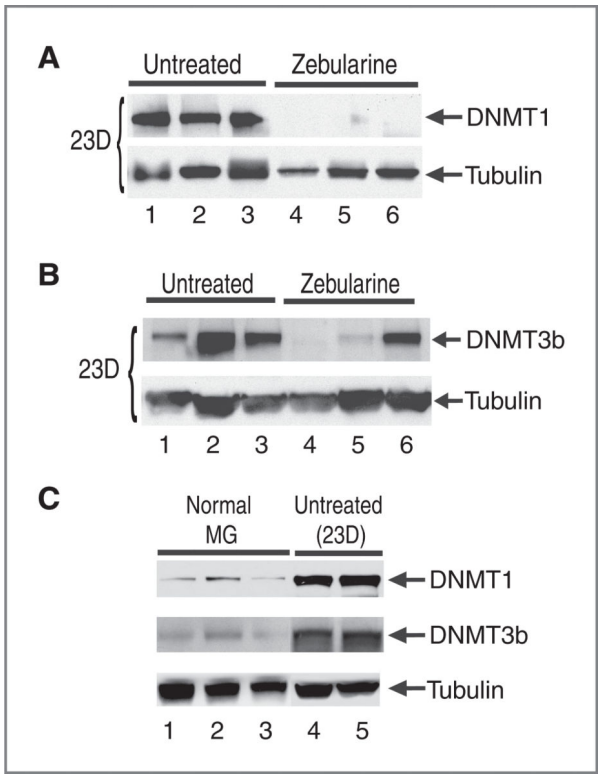

Figure 3.

Depletion of DNMT1 and DNMT3b in zebularine-treated transgenic mice. A, immunoblot analysis of DNMT1. Tumors from both untreated (n = 3; lanes 1–3) and zebularine-treated mice (n = 3; lanes 4–6) were isolated after 23 days of treatment. B, immunoblot analysis of DNMT3b from untreated tumors (n = 3; lanes 1–3) and zebularine-treated mice (n = 3; lanes 4–6). C, immunoblot analysis of DNMT1 and DNMT3b from lysates isolated from normal mammary gland 4 (lanes 1–3) as compared with additional untreated tumor specimens (lanes 4 and 5). α-Tubulin was used as a protein loading control. MG, mammary gland.

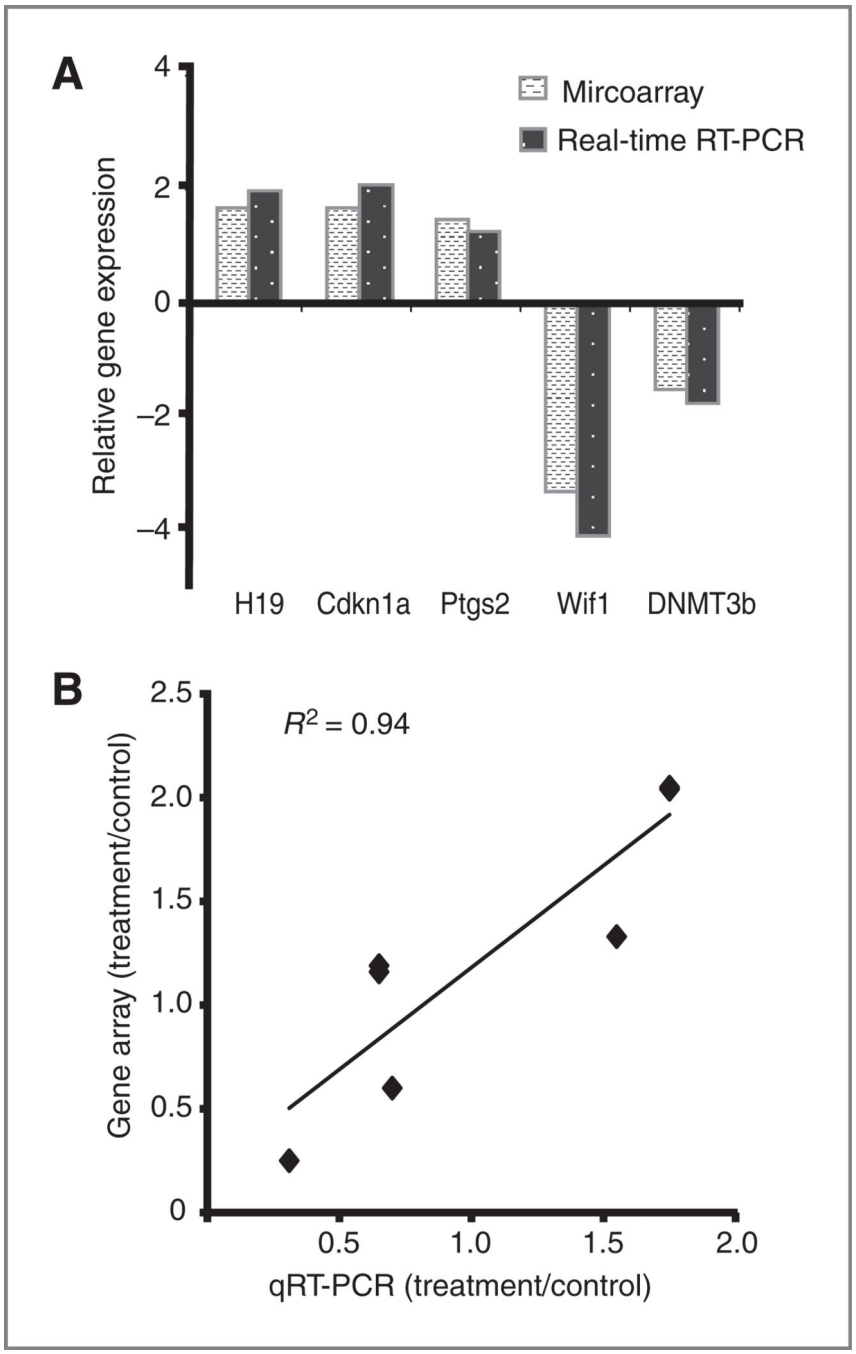

Figure 4.

Validation of microarray analysis of zebularine-regulated gene expression by real-time RT-PCR. A, comparison of the relative fold change of zebularine-regulated genes as measured by microarray or quantitative real-time RT-PCR. B, positive correlation between real-time RT-PCR and microarray analysis of zebularine-regulated genes (R^2 = 0.94).

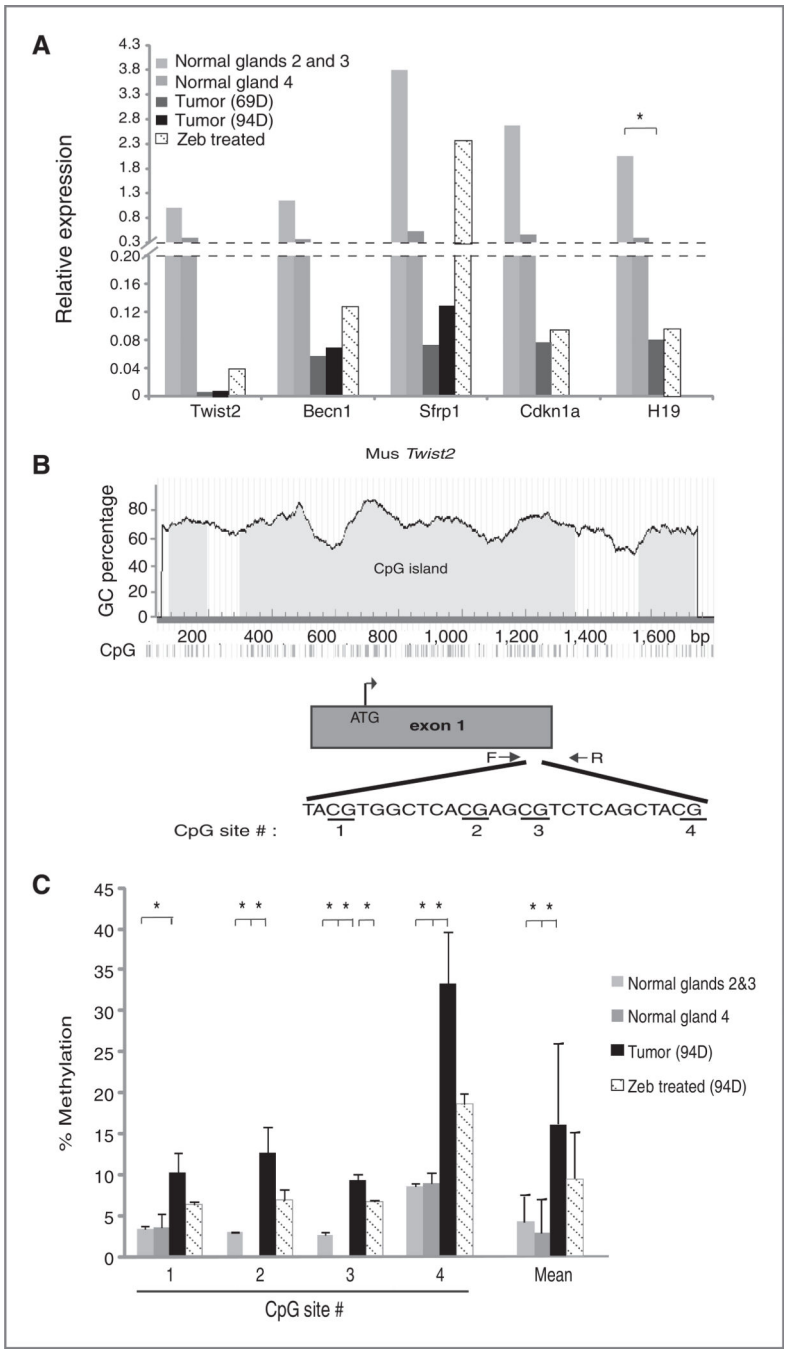

Figure 5.

The mRNA expression level and methylation status of selected zebularine-activated genes are altered during mammary tumor development and zebularine treatment. A, quantitative RT-PCR measurement of Twist2, Becn1, Sfrp1, Cdkn1a, and H19 expression in normal mammary glands 2 and 3 and 4 measured independently from 70-day-old FVB mice, mammary tumors from 69-day-old and 94-day-old PyMT transgenic mice, and tumor samples from zebularine-treated PyMT mice [69-day for all genes except 94-day for Twist2; 69 and 94 days corresponds to 23 and 48 days after zebularine (Zeb) treatment,

respectively]. Each bar represents the mean gene expression level measured in 3 individual mice. B, the architecture of the mouse *Twist2* locus. Included is the GC percentage and location of exon 1 within this locus, the transcriptional start site (ATG), location of PCR primers used to amplify a portion of the *Twist2* gene, and the gene sequence and individual CpG dinucleotides interrogated by pyrosequencing. C, The percentage of methylated CpG dinucleotides within the *Twist2* gene in indicated tissue or tumor samples measured by pyrosequencing. Measurements in normal mammary glands 2 and 3 and 4 from control FVB mice are graphed separately. Each bar indicates mean methylation of the indicated CpG dinucleotide within the *Twist2* gene, measured in 3 independent tissue or tumor samples (error bars, ± SE). Also graphed is the average CpG methylation at all 4 CpG sites analyzed. Statistical test used was a 2-tailed *t* test comparing normal mammary glands or zebularine-treated tumors to untreated tumors (*, $P < 0.05$).

Table 1.

Upregulated genes in tumors isolated from zebularine-treated mice

			Ratio of zebularine/control			Functional groups by Gene Ontology			
Gene ID	**Gene symbol**	**Gene name**	**13 d[a]**	**23 d[a]**	**48 d[a]**	**Cell cycle**	**Methylation and methylated genes**	**Apoptosis**	**Negative regulation of cell proliferation**
AV310588	*Ccnd2*	Cyclin D2	1.58			+	+		+
AK007630	*Cdkn1a*	Cyclin-dependent kinase inhibitor 1A (p21)		1.76		+	+		+
AV238225	*Lmna*	Lamin A		1.54		+	+		
BG095529	*Becn1*	Beclin 1 (coiled-coil, myosin-like BCL2-interacting protein)		2.35			+		+
NM_023123	*H19*	H19 fetal liver mRNA		1.75			+		
NM_009369	*Tgfβi*	Transforming growth factor, beta induced		1.51			+		
M94967	*Ptgs2*	Prostaglandin-endoperoxide synthase 2		1.56			+		
BI658627	*Sfrp1*	Secreted frizzled-related sequence protein 1			1.68		+	+	+
AV025667	*Gsn*	Gelsolin			1.56		+		
NM_007855	*Twist2*	Twist homolog 2 (Drosophila)			2.39		+		
NM_010866	*Myod1*	Myogenic differentiation 1			1.73		+		
NM_008344	*Igfbp6*	Insulin-like growth factor binding protein 6			1.64		+		
NM_007609	*Casp4*	Caspase 4, apoptosis-related cysteine protease		2.04				+	

[a]Days of zebularine treatment.

Table 2.

Downregulated genes in tumors isolated from zebularine-treated mice

Gene ID	Gene symbol	Gene name	Ratio of zebularine vs. control			Functional group by Gene Ontology						
			13 d[a]	23 d[a]	48 d[a]	Cell cycle	Methylation and methylated genes	Metastasis	Positive regulation of cell proliferation	AKT/ PI3K-signaling	Src-signaling	RAS-signaling
NM_009870	*Cdk4*	Cyclin-dependent kinase 4	0.66			+			+			
BB209183	*Cdc25C*	Cell division cycle 25 homolog C (S. cerevisiae)	0.65			+			+			
NM_023223.2	*Cdc20*	Cell division cycle 20 homolog (S. cerevisiae)	0.65			+			+			
NM_008566.2	*Mcm5*	Minichromosome maintenance deficient 5, cell division cycle 46 (S. cerevisiae)	0.59			+			+			
BI658327.1	*Mcm3*	Minichromosome maintenance deficient 3 (S. cerevisiae)	0.67			+			+			
NM_008569.2	*Anapc1*	Anaphase promoting complex subunit 1		0.55		+			+			
BB828014	*Trp53*	Transformation related protein 53	0.54			+			+			
BB183559	*Hdac11*	Histone deacetylase 11		0.59			+					
BC004048	*Wif1*	Wnt inhibitory factor 1			0.31		+					
BC019135	*Mmp12*	Matrix metalloproteinase 12		0.47				+				
NM_008607	*Mmp13*	Matrix metalloproteinase 13			0.28			+				
M94335	*Akt1*	Thymoma viral proto-oncogene 1	0.66						+	+		
BB207248	*Pik3cd*	Phosphatidylinositol 3-kinase catalytic delta polypeptide		0.44							+	
U52193	*Pik3c2a*	Phosphatidylinositol 3-kinase, C2 domain containing, alpha polypeptide		0.66							+	
NM_007615	*Catns*	Catenin src	0.54					+			+	
AK020374	*Tnfrsf11a*	Tumor necrosis factor receptor superfamily, member 11a	0.63									+
NM_013869	*Tnfrsf19*	Tumor necrosis factor receptor superfamily, member 19		0.66								+

Gene ID	Gene symbol	Gene name	Ratio of zebularine vs. control			Functional group by Gene Ontology						
			13 d[a]	23 d[a]	48 d[a]	Cell cycle	Methylation and methylated genes	Metastasis	Positive regulation of cell proliferation	AKT/ PI3K-signaling	Src-signaling	RAS-signaling
NM_013832	*Rasal1*	RAS protein activator like 1 (GAP1 like)	0.61									+

[a]Days of zebularine treatment.